



EUROPEAN ORGANISATION FOR NUCLEAR RESEARCH

CERN-EP/86-88

CHARM PRODUCTION IN DEEP INELASTIC MUON-IRON

10 July 1986

INTERACTIONS AT 200 GeV/c

The European Muon Collaboration

CERN<sup>1</sup>, DESY (Hamburg)<sup>2</sup>, Freiburg<sup>3</sup>, Kiel<sup>4</sup>, Lancaster<sup>5</sup>, LAPP (Annecy)<sup>6</sup>,  
Liverpool<sup>7</sup>, Marseille<sup>8</sup>, Oxford<sup>9</sup>, Rutherford<sup>10</sup>, Sheffield<sup>11</sup>,  
Turin<sup>12</sup>, Wuppertal<sup>13</sup>.

M. Arneodo<sup>12</sup>, J.J. Aubert<sup>8</sup>, G. Bassompierre<sup>6</sup>, K.H. Becks<sup>13</sup>, C. Benchouk<sup>8</sup>,  
C. Best<sup>10a)</sup>, E. Böhm<sup>4</sup>, X. de Bouard<sup>6</sup>, F.W. Brasse<sup>2</sup>, C. Broll<sup>6+</sup>,  
S.C. Brown<sup>7b)</sup>, J. Carr<sup>10c)</sup>, R. Clifft<sup>10</sup>, J.H. Cobb<sup>5d)</sup>, G. Coignet<sup>6</sup>,  
F. Combley<sup>11</sup>, G.R. Court<sup>7</sup>, G. D'Agostini<sup>8</sup>, W.D. Dau<sup>4</sup>, J.K. Davies<sup>9e)</sup>,  
Y. Déclais<sup>6f)</sup>, U. Dosselli<sup>13g)</sup>, J. Drees<sup>13</sup>, A. Edwards<sup>13a)</sup>, M. Edwards<sup>10</sup>,  
J. Favier<sup>6</sup>, M.I. Ferrero<sup>12</sup>, W. Flauger<sup>2</sup>, H. Forsbach<sup>13</sup>, E. Gabathuler<sup>7</sup>,  
R. Gamet<sup>7</sup>, J. Gayler<sup>2</sup>, V. Gerhardt<sup>2h)</sup>, C. Gössling<sup>2i)</sup>, J. Haas<sup>3</sup>,  
K. Hamacher<sup>13</sup>, P. Hayman<sup>7</sup>, M. Henckes<sup>13j)</sup>, V. Korbel<sup>2</sup>, U. Landgraf<sup>3</sup>,  
M. Leenen<sup>1k)</sup>, M. Maire<sup>6</sup>, S. Maselli<sup>12l)</sup>, W. Mohr<sup>3</sup>, H.E. Montgomery<sup>1m)</sup>,  
K. Moser<sup>3n)</sup>, R.P. Mount<sup>9o)</sup>, E. Nagy<sup>6p)</sup>, J. Nassalski<sup>2q)</sup>, P.R. Norton<sup>10</sup>,  
J. McNicholas<sup>9r)</sup>, A.M. Osborne<sup>1</sup>, P. Payre<sup>8</sup>, C. Peroni<sup>12</sup>, H. Pessard<sup>6</sup>,  
U. Pietrzyk<sup>13</sup>, K. Rith<sup>9s)</sup>, M. Schneegans<sup>6</sup>, T. Sloan<sup>5</sup>, H.E. Stier<sup>3</sup>,  
W. Stockhausen<sup>13t)</sup>, J.M. Thénard<sup>6</sup>, J.C. Thompson<sup>10</sup>, L. Urban<sup>6p)</sup>,  
H. Wahlen<sup>13</sup>, M. Whalley<sup>11u)</sup>, D. Williams<sup>7v)</sup>, W.S.C. Williams<sup>9</sup>,  
J. Williamson<sup>11w)</sup>, S.J. Wimpenny<sup>7i)</sup>.

### Abstract

Dimuon and trimuon events have been studied in deep inelastic muon scattering on an iron target at an incident muon energy of 200 GeV. The events are shown to originate mainly from charm production. Comparison of the measured cross sections with data taken at higher muon energies shows that charm production originates predominantly from transverse virtual photons. Within the framework of the photon gluon fusion model this indicates that the parity of the gluon is odd.

(Submitted to Zeits. für Physik C)

---

For footnotes see next page.

- a) Now at JET, Joint Undertaking, Abingdon, England.
- b) Now at TESSA, Lausanne, Switzerland.
- c) Now at University of Colorado, Boulder, Colorado, USA.
- d) Now at University of Oxford, England
- e) Now at Plessey Defence Systems, Fareham, England.
- f) Now at Université d'Aix-Marseille II, Luminy, France.
- g) Now at INFN. Sez. Padova, Italy.
- h) Now at Beiersdorf AG, Hamburg, Germany.
- i) Now at CERN, Geneva, Switzerland.
- j) Now at ICR-PV, Köln, Germany.
- k) Now at DESY, Hamburg, Germany.
- l) Now at Max-Planck-Institut, Munich, Germany.
- m) Now at FNAL, Batavia, Illinois, U.S.A.
- n) Now at Fraunhofer Gesellschaft, Stuttgart, Germany.
- o) Now at California Institute of Technology, Pasadena, California, USA.
- p) Now at Central Research Institute for Physics of the Hungarian Academy of Science, Budapest, Hungary.
- q) Now at Institute for Nuclear Studies, Warsaw, Poland.
- r) Now at GEC Computers, Coventry, England.
- s) Now at MPI, Heidelberg, Germany.
- t) Now at SLAC, Stanford, California, U.S.A.
- u) Now at Durham University, Durham, England.
- v) Now at U.K.A.E.A., Winfrith, Dorchester, England.
- w) Now at RAL, Chilton, Didcot, Oxon, England.
- i) Now at CERN, Geneva, Switzerland.
- + ) Deceased.

## Introduction

In previous publications [1,2] dimuon and trimuon events were studied in 250 and 280 GeV muon-iron interactions. The dominant source of these events was shown to be the production of charmed particles, which then decayed semi-leptonically into muons. Similar data taken at a lower beam energy (200 GeV), are presented in this paper. Combined with the 250 GeV data [1] they provide a measurement of  $R = \sigma_L/\sigma_T$  for charm production in deep inelastic muon scattering, where  $\sigma_L$  and  $\sigma_T$  are the cross sections for charm production by longitudinally and transversely polarised virtual photons, respectively.

Such a measurement is interesting as it can distinguish between different gluon spin-parity,  $J^P$ , assignments. This arises from the assumption, confirmed by the data, that photon gluon fusion [3] is the principal mechanism responsible for charm production in deep inelastic scattering. The process under study is then directly proportional to the gluon component of the nucleon wave function. It can thus be shown [4] that  $1^-$  and  $0^-$  spin parity assignments lead to a dominantly (or completely in the  $0^-$  case) transverse cross section, implying a small value of  $R$ . Even parity gluons ( $0^+$ ,  $1^+$ ) on the other hand, lead to large longitudinal contributions which imply very large values of  $R$  (e.g.  $R$  becomes infinite for  $J^P = 1^+$ ). Data from  $e^+e^-$  experiments [5] which studied the distributions on the Dalitz plot of 3 jet events favour vector gluons as expected from QCD.

The usual kinematic variables of deep inelastic scattering will be used. These are  $Q^2 (= -q^2)$ , the four momentum squared,  $\nu$ , the energy transferred in the laboratory frame to the virtual photon,  $x_{Bj} = Q^2/2M\nu$ , the Bjorken variable,  $y = \nu/E_{beam}$ , and  $z = E_\mu/\nu$ , where  $E_\mu$  is the energy of the decay muon.

## Experimental Apparatus and Data Analysis

The experiment was performed in the M2 beam line at the CERN SPS using the EMC forward spectrometer, already described elsewhere [6]. Muons were

incident on a target consisting of an iron-scintillator shower total absorption calorimeter (STAC) [7] with total thickness of approximately  $1,600 \text{ g/cm}^2$ . Events were selected in the upstream 2m of the target, leaving at least 4 absorption lengths of material in the target downstream from the interaction vertex. This requirement minimised the contamination from  $\pi$  and K mesons leaking from the shower in the target calorimeter and decaying to muons in the forward spectrometer region. It also ensured that the whole hadronic shower was absorbed in the STAC, so that a reliable energy measurement could be made. Two data sets (at 200 GeV incident muon energy) were taken, one with positive and one with negative incident muons ( $3.9 \times 10^{10}$ ,  $4.0 \times 10^{10}$  muons respectively), corresponding to a total luminosity of  $5.2 \times 10^{37} \text{ cm}^{-2}$ . These data sets, which were compatible within their statistical errors, were combined in the analysis presented here.

The analysis procedures and data reduction for the multimMuon events were identical to those described in [1]. We will focus mainly on the dimuon events. As explained below, the trimuon events were useful to provide consistency checks of the dimuon sample, within the constraints imposed by their limited statistics.

As shown in [1,2] the missing energy associated with the multimMuon events provides a signature for charm production. This missing energy is assumed to be carried away by neutrinos. For charm production the missing energy is larger than that expected from the decay of  $\pi$  and K mesons produced in ordinary deep inelastic scattering events.

The missing energy,  $E_{\text{miss}}$ , is defined as the difference between the incident muon energy,  $E_{\text{beam}}$ , and the sum of the observed energy in the muon tracks,  $E_{\mu}$ , as measured in the forward spectrometer and the hadron shower energy  $E_{\text{STAC}}$  measured in the target calorimeter:

$$E_{\text{miss}} = E_{\text{beam}} - \sum_i E_{\mu_i} - E_{\text{STAC}} \quad \begin{array}{l} i = 1,2 \quad \text{for dimuons} \\ i = 1,2,3 \quad \text{for trimuons} \end{array}$$

Electromagnetic tridents, in which one of the muons escapes detection, were removed from the data sample. This was accomplished by requiring that

the missing energy be less than 60 GeV (thereby eliminating the electromagnetic events in which the missing energy includes the energy of the scattered, undetected muon) and that the energy deposited in the STAC target be larger than 15 GeV, thus rejecting elastic events. This background was further reduced by rejecting those events which appeared to have a third muon in the beam region, signalled by an extra hit in the downstream hodoscope H5 (used for monitoring the beam intensity) or an extra track in the proportional chamber P0, in the beam region [6].

In order to reduce the contributions from  $\pi$  and K meson decays and to avoid regions where the acceptance was either too small or rapidly changing, the following kinematic cuts were applied:  $Q^2 > 1 \text{ GeV}^2$ ,  $15 \text{ GeV} < \nu < 185 \text{ GeV}$ ,  $y(= \nu/E_{\text{beam}}) < 0.85$  (this allowed radiative corrections to be neglected), scattered muon momentum greater than 15 GeV and decay muon momentum greater than 12.5 GeV. The data samples after these selections were as follows: 294  $\mu^+ \mu^-$  and 257  $\mu^+ \mu^+$  events for the incident  $\mu^+$  data and 297  $\mu^- \mu^+$  and 314  $\mu^- \mu^-$  events for the incident  $\mu^-$  data.

Figure 1 shows the measured distribution of the missing energy for the dimuon events together with an absolute Monte Carlo calculation giving the distribution expected from  $\pi$  and K decays (see below). The observed mean value of  $13.5 \pm 2.0 \text{ GeV}$  compared to that expected from  $\pi$ , K decay of 5.5 GeV shows that a large proportion of the events originates from a different source such as charm production. From the ratio of the number of trimuon events to that of dimuon events, after correcting for the different acceptances and  $\pi$ , K decay background, the mean semileptonic branching ratio for D mesons can be computed. The result  $(11 \pm 5)\%$  is consistent with the published value<sup>†</sup>  $8.2 \pm 1.2\%$  [8]. The multimMuon events, selected by the procedure described below, therefore appear to originate predominantly from the production and semileptonic decay of charmed D mesons.

<sup>†</sup> More recent measurements by the Mark III collaboration at SLAC indicate that all the previously measured charmed particle branching ratios have been underestimated by ~50%. However, as discussed later, the old value of the mean semileptonic branching ratio is used throughout this analysis to allow comparison with the previous measurements.

The data were then corrected for the calculated  $\pi/K$  decay background which amounts to  $(42 \pm 20)\%$  of the total observed dimuon events. A Monte Carlo programme [9] to model the hadronic shower development was used to calculate this. The larger fraction of  $\pi/K$  events, compared to the data discussed in [1,2], is a consequence of the smaller cross section for charm production at the lower beam energy and to the reduced momentum cut for the final state decay muons. Corrections were also applied for P0-H5 random vetoing as explained in [1] and the residual electromagnetic background. They amounted to a few percent (P0-H5:  $6\% \pm 2\%$ , tridents:  $2\% \pm 2\%$  in the  $\mu^+ \mu^-$  sample only).

Cross sections for charm production were extracted from the data as follows. A Monte Carlo programme was used to compute the acceptance. This simulated the experimental setup, including hodoscope and chamber efficiencies and resolution. This programme generated events according to the photon-gluon fusion model [3] which gave a good representation of the 250 and 280 GeV data [1,2]. The parameters used for the model were those optimised for the 250 GeV data [1]. In particular, the charm fragmentation function used was the best fit obtained in [1]. The Monte Carlo calculations were repeated for each of the data sets with incident  $\mu^+$  and  $\mu^-$ .

The generated Monte Carlo events were tracked through the apparatus. Each generated event was accepted if it fulfilled the trigger requirement and would have been detected in the forward spectrometer. The ratio of the accepted to the generated weight in a given bin gave the apparatus acceptance in that bin.

The data taken with positive and negative beam muons were analysed separately. In both cases it was found that the differential cross sections for events with same sign and opposite sign muons in the final state were consistent within the statistical errors. The two sets of events (same sign and opposite sign dimuons) were therefore combined. Furthermore, the cross sections extracted from the two data sets with different beam sign also proved to be consistent with each other. They were averaged and the results are presented below. It should be noted that the apparatus is only sensitive to the forward region in the centre of mass frame.

Figures 2 give the differential cross sections for muon production of charm ( $\mu N \rightarrow \mu c \bar{c} X$ ) as a function of  $Q^2$ ,  $x_{Bj}$  and  $z$ , in the range  $Q^2 > 1 \text{ GeV}^2$  assuming a mean semileptonic branching ratio of  $8.2 \pm 1.2\%$  [8]. The point at the lowest  $Q^2$  has a large systematic uncertainty ( $\sim 100\%$ ) due to the large decay corrections in this region and uncertainties in the acceptance. The smooth curves show the predictions of the photon gluon fusion model. As in the data at higher energies this model gives a good representation of the data. The error bars shown are statistical errors only.

From the measured cross sections for  $\mu N \rightarrow \mu c \bar{c} X$ , the photoproduction cross sections for the process  $\gamma^* N \rightarrow c \bar{c} X$  were calculated as follows:

$$\frac{d^2\sigma}{dQ^2 dv}(\mu N \rightarrow \mu c \bar{c} X) = \Gamma (\sigma_T + \epsilon \sigma_L) \quad (1)$$

with

$$\Gamma = \frac{\alpha(v - Q^2/2M)}{2\pi Q^2 E_{\text{beam}}^2 (1 - \epsilon)}$$

and

$$\epsilon = \left[ 1 + \frac{Q^2 + v^2}{2E_{\text{beam}} E' - Q^2/2} \right]^{-1}, \quad (2)$$

where  $E' = E_{\text{beam}} - v$ , the energy of the scattered muon.

Table 1 gives  $\sigma(\gamma^* N \rightarrow c \bar{c} X)$ , the cross section  $\sigma_T + \epsilon \sigma_L$ , for the 200 GeV data.

$\sigma(\gamma^* N \rightarrow c \bar{c} X)$  can then be extrapolated to  $Q^2 = 0$ , thereby obtaining the cross section for production of open charm by real photons. Figure 3 shows the results obtained by using the same method as in [1]. The inner error bars are statistical and the outer are systematic. The systematic errors essentially arose from the estimated systematic uncertainty on the  $\pi/K$  decay contribution and from the uncertainty of the fragmentation function. The systematic error on the flux gives a negligible contribution. The results are presented together with the multimMuon data [10],  $D^0$  production data [11] and photoproduction experiment data [12-14]. The smooth curve shows the absolute prediction of the photon gluon fusion model. There is good agreement within the errors between the data presented here, the results of the other experiments [1,10-14] and the predictions of this model.

All the data in fig. 3 were computed using the old branching ratios [8] for charm production. As noted above, the Mark III collaboration at SLAC [15], using tagged charmed particles, observe branching ratios which are about 50% greater than the old values. The previous values required the absolute values of the charmed production cross sections in  $e^+e^-$  annihilation and these had presumably been overestimated. Thus all the cross sections in fig. 3 should be reduced correspondingly. This is also true for the values of  $F_2^{cc}$ , the contribution of charm to the nucleon structure function  $F_2$ , given in [1]. The fits [1] of the data to the photon gluon fusion model gave rather large values of  $\alpha_s$ , the strong coupling constant, and hence of  $\Lambda$ , the QCD mass scale parameter. Using the new values of the mean semileptonic branching ratio would give lower values of these quantities which are more consistent with other measurements [16].

The cross section for  $\gamma^*N \rightarrow c\bar{c}X$  can be written as

$$\sigma(\gamma^*N \rightarrow c\bar{c}X) = \sigma_T(Q^2, \nu) (1 + \epsilon R) \quad (3)$$

where  $R = \sigma_L/\sigma_T$  and  $\sigma_L, \sigma_T$  are functions of  $Q^2, \nu$  only. It then becomes possible to extract R from the values of  $\sigma(\gamma^*N \rightarrow c\bar{c}X)$  measured at the two different beam energies (200 and 250 GeV [1]). We can write (3) for the two data sets,

$$\sigma^{(200)} = \sigma_T(Q^2, \nu) (1 + \epsilon^{(200)} R) \quad (4)$$

$$\sigma^{(250)} = \sigma_T(Q^2, \nu) (1 + \epsilon^{(250)} R) .$$

where for a fixed  $Q^2$  and  $\nu$ ,  $\sigma_T$  is the same for the two beam energies. For a given  $(Q^2, \nu)$  bin equation (4) can then be solved for R. This gives:

$$R = \frac{\sigma^{(250)} - \sigma^{(200)}}{\epsilon^{(250)} \sigma^{(200)} - \epsilon^{(200)} \sigma^{(250)}}$$



The calculation of  $R$  was carried out in the part of the  $Q^2, \nu$  plane where the two data samples overlap, excluding regions of small acceptance ( $< 5\%$  and  $< 1\%$  for the 200 and for the 250 GeV data sets respectively). The 250 GeV data are given in table IVa of [1].

Table 2 shows the values thus obtained. They were averaged neglecting any  $Q^2, \nu$  dependence of  $R$ . The final result is

$$R = - 0.6 \pm 0.2 \text{ (stat.)} \pm 0.4 \text{ (syst.)} .$$

The systematic uncertainty of the result originates mainly from the relative normalisation error of the two data sets, from the systematic error on the  $\pi$ ,  $K$  decays and from the non-uniformity of the bin populations. The error due to the fragmentation function is assumed to cancel.

The result is consistent with  $R = 0$  and with previous measurements in deep inelastic scattering experiments [17]. The result implies that  $R < 0.3$  at 90% confidence level. It should be emphasised however that  $R = \sigma_L / \sigma_T$  as measured in charm production need not be the same as that observed in single arm deep inelastic scattering, to which it contributes about 1% only. The mechanism which determines  $R$  for charm production is different from that which influences  $R$  for single arm deep inelastic scattering.

As discussed above, a measurement of  $R$  allows the different gluon spin-parity assignments to be distinguished. The measured value of  $R$ , which is consistent with zero within the errors, is consistent with odd parity gluons:  $0^-$  or  $1^-$ , the latter being the QCD prediction. However, it disfavours even parity assignments (large  $R$ ) [4]. In particular it excludes axial vector gluons, for which  $\sigma_T = 0$ , corresponding to an infinite value of  $R$ .

In conclusion, charm production in 200 GeV muon-iron interactions has been studied. The results have been shown to be consistent with those obtained from higher energy data (250 GeV) and with the photon gluon fusion model. By combining the two data sets a value for  $R = \sigma_L / \sigma_T$  has been obtained, showing that charm production in deep inelastic muon scattering can be predominantly ascribed to transversely polarised virtual photons. The value obtained for  $R$  is consistent with the QCD spin parity assignment for the gluon within the framework of the photon gluon fusion model.

References

- [1] EMC, J.J. Aubert et al., Nucl. Phys. B213 (1983) 1.
- [2] EMC, J.J. Aubert et al., Phys. Lett. 94B (1980) 96;  
EMC, J.J. Aubert et al., Phys. Lett. 94B (1980) 101.
- [3] J. Leveille and T. Weiler, Nucl. Phys. B147 (1979) 147.
- [4] T. Weiler, Phys. Rev. Lett. 44 (1980) 304.
- [5] TASSO, R. Brandelik et al., Phys. Lett. 97B (1980) 453;  
CELLO, H.J. Behrend et al., Phys. Lett. 110B (1982) 329;  
PLUTO, Ch. Berger et al., Phys. Lett. 119B (1982) 239.
- [6] EMC, O.C. Allkofer et al., Nucl. Instr. and Meths. 179 (1981) 445.
- [7] V. Korbel, Proceedings of the XIVth Rencontre de Moriond (1979),  
Vol. II, ed. Tran Thanh Van.
- [8] Particle Data Table, Rev. Mod. Phys. 52 (1980).
- [9] A. Grant, Nucl. Instr. and Meths. 131 (1975) 167.
- [10] BFP, A.R. Clark et al., Phys. Rev. Lett. 45 (1980) 686.
- [11] EMC, J.J. Aubert et al., Phys. Lett. 167B (1986) 127.
- [12] K. Abe et al., Phys. Rev. Lett. 51 (1983) 156.
- [13] WA4, D. Aston et al., Phys. Lett. 94B (1980) 113.
- [14] CIF, M.S. Atiya et al., Phys. Rev. Lett. 43 (1979) 414.
- [15] Mark III, R.M. Baltrusaitis et al., Phys. Rev. Lett. 54 (1985) 1976.
- [16] D.W. Duke, R.G. Roberts, Phys. Rep. 120 (1985) 275.
- [17] See for example J. Drees and H.E. Montgomery, Ann. Rev. Nucl. Sci. 33 (1983): 383-452 and references cited therein.

Table 1

$\sigma(\gamma^*N \rightarrow c\bar{c}X)$  (nb)  
Beam Energy 200 GeV

$Q^2$ (GeV <sup>2</sup> )	1.0	1.78	3.16	5.62	10.0	17.8	31.6
	-1.78	-3.16	-5.62	-10.0	-17.8	-31.6	-56.2
$\nu$ (GeV)	-	-	-	-	-	-	-
40-60	-	-	212±236	-	14±27	-	-
60-80	-	-	281±235	415±383	276±289	-	-
80-100	-	344±430	187±79	199±59	95±41	56±72	12±28
100-120	-	171±164	307±80	343±80	211±54	38±25	-
120-140	-	536±152	433±82	239±53	170±51	45±33	82±91
140-160	922±253	670±144	441±76	374±75	272±74	114±46	45±56
160-180	1309±515	621±218	437±144	508±149	205±82	223±326	-

Table 2

Values of R

$Q^2$ (GeV <sup>2</sup> ) $\nu$ (Gev)	3.16 - 10	10 - 31.6
120-160	$-0.3 \pm 0.4$	$-0.7 \pm 0.3$
160-200	$-0.9 \pm 0.4$	$-0.7 \pm 1.7$

Figure Captions

Fig. 1 Missing energy distribution for the final sample of dimuon events. The distribution labelled  $\pi/K$  is the calculated background from  $\pi/K$  decays in hadron showers from deep inelastic scattering events.

Fig. 2 Differential cross sections for muon production of charm in the range  $Q^2 > 1 \text{ GeV}^2$ . The smooth line is the photon gluon fusion model prediction.

a)  $\frac{d\sigma}{dQ^2} (\mu N \rightarrow \mu c \bar{c} X)$

b)  $\frac{d\sigma}{dx_{Bj}} (\mu N \rightarrow \mu c \bar{c} X)$

c)  $\frac{d\sigma}{dz} (\mu N \rightarrow \mu c \bar{c} X)$

Fig. 3 The total charm photoproduction cross section ( $Q^2=0$ ) as a function of the photon energy.

- o This experiment (EMC) in  $\gamma_V^* + \text{Fe} \rightarrow c \bar{c} X$  (inner error bars are statistical, outer error bars are systematic)
- ▼ EMC MultimMuon results [1] in  $\gamma^* + \text{Fe} \rightarrow c \bar{c} + X$
- EMC results [11] in  $\gamma^* + \text{N} \rightarrow D^0(\bar{D}^0) + X$
- ∇ BFP MultimMuon results [10] in  $\gamma^* + \text{Fe} \rightarrow c \bar{c} + X$
- Δ SLAC results [12] in  $\gamma + p \rightarrow c \bar{c} + X$
- X WA4 Collaboration [13] in  $\gamma + p \rightarrow \bar{D}^0 + X$
- CIF FNAL [14] in  $\gamma + (\text{CH}) \rightarrow D^0(\bar{D}^0) + X$

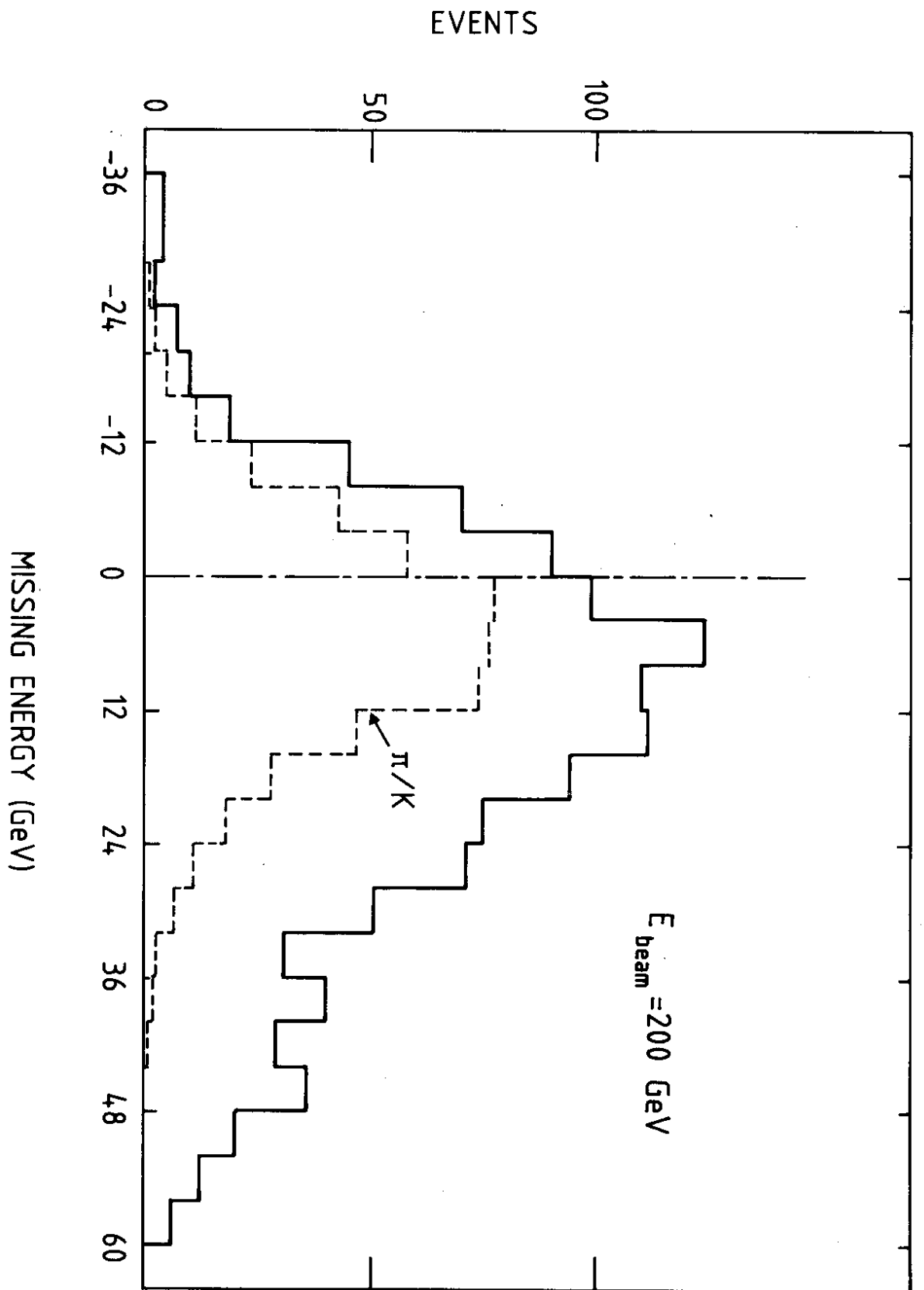


FIG. 1

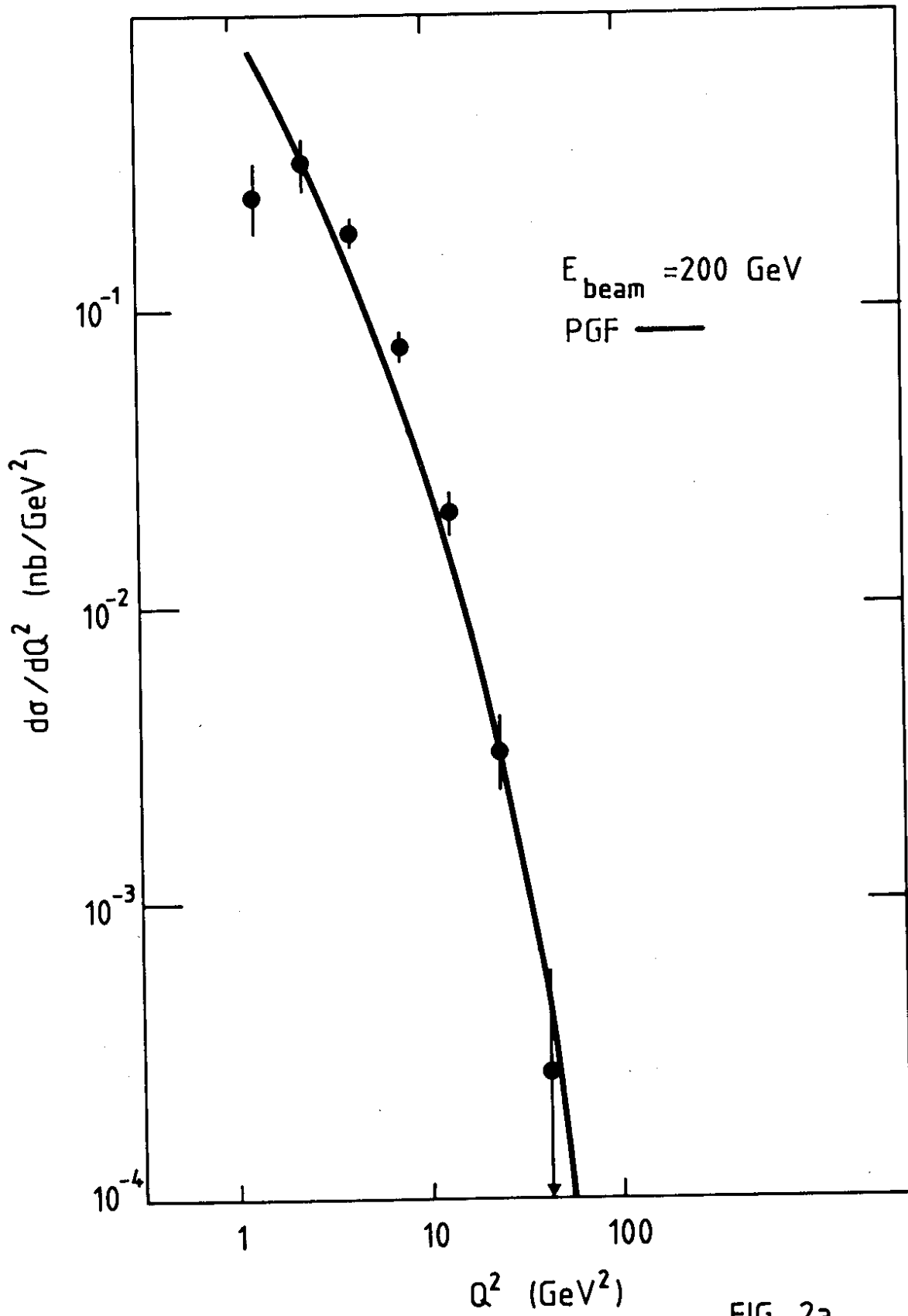
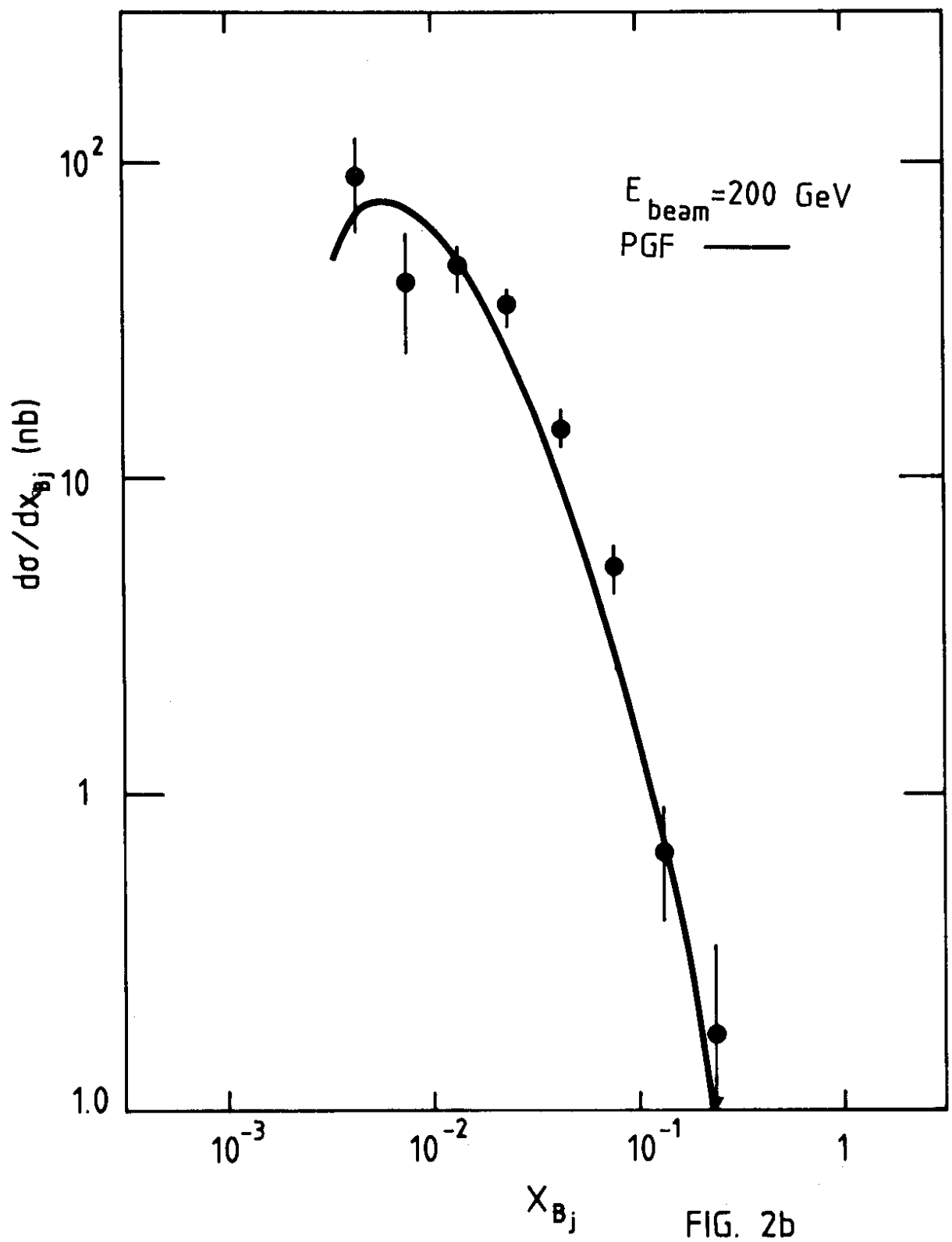


FIG. 2a





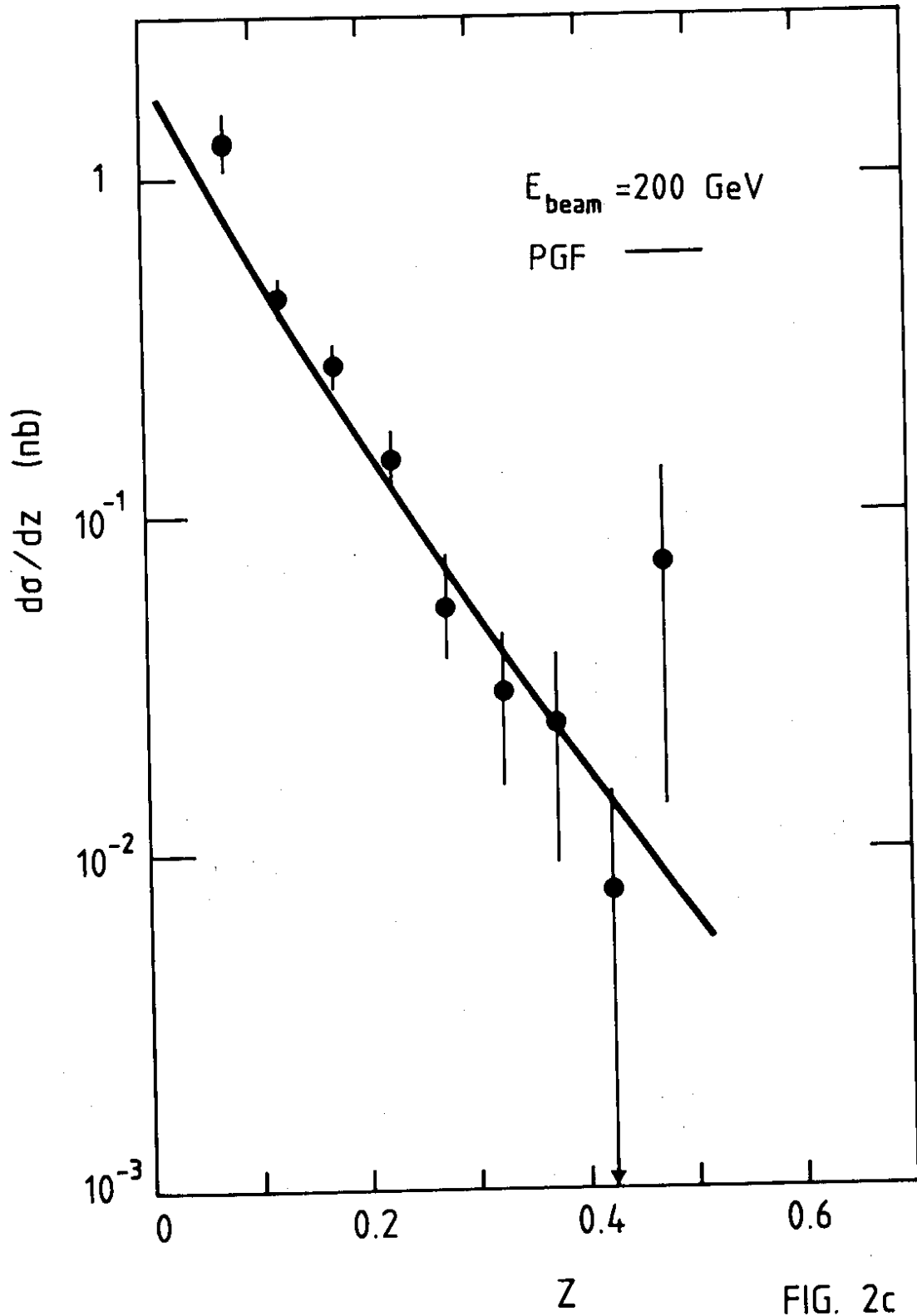


FIG. 2c

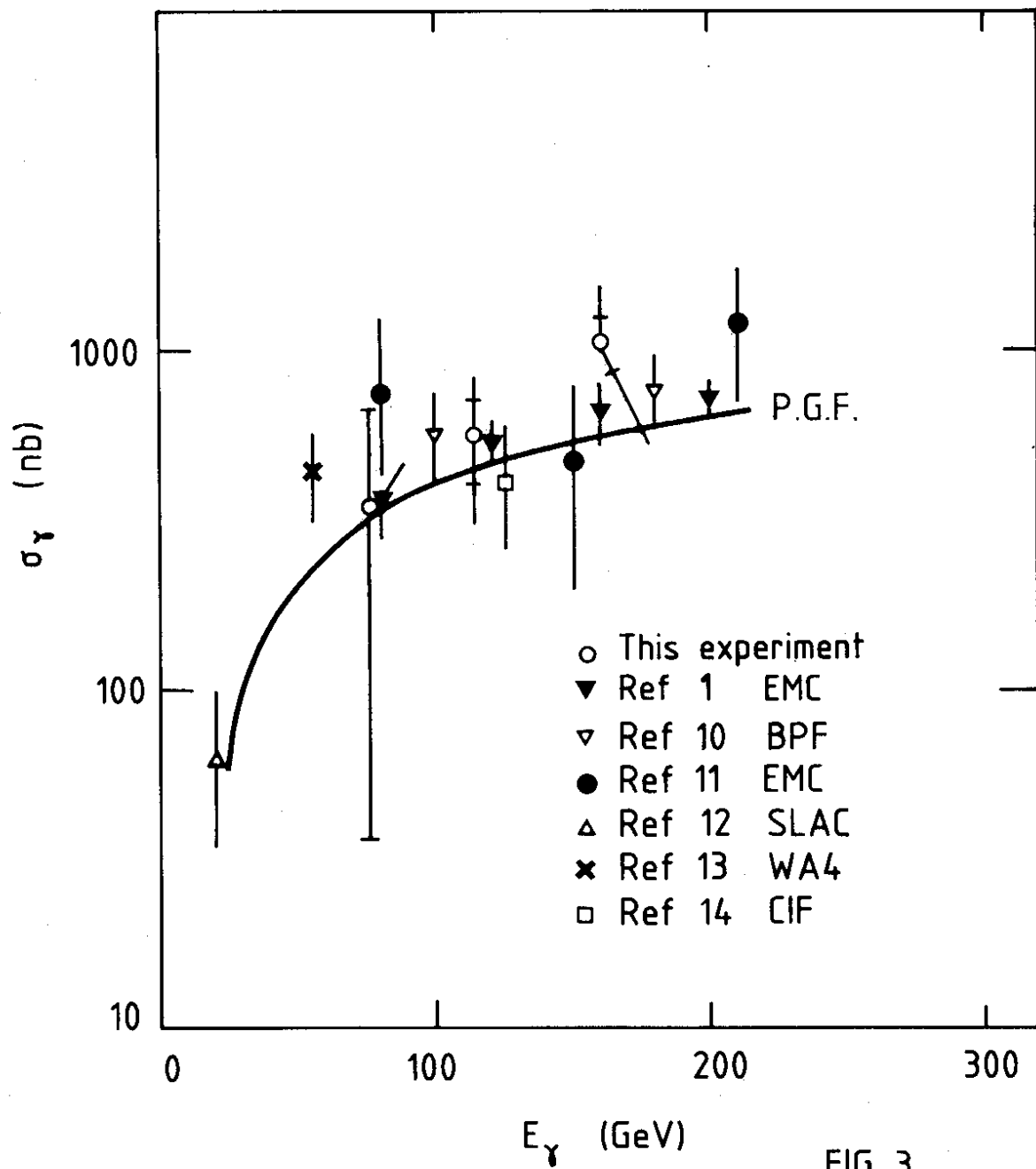


FIG. 3